

Towards high power broad-band OPCPA at 3000 nm

M. BRIDGER^{*}, O. A. NARANJO-MONTOYA, A. TARASEVITCH^{**}, AND U. BOVENSIEPEN

University of Duisburg-Essen, Faculty of Physics, Lotharstrasse 1, 47057 Duisburg, Germany

**manuel.bridger@uni-due.de*

***alexander.tarasevitch@uni-due.de*

Abstract: High-energy femtosecond laser pulses in the mid-infrared (MIR) wavelength range are essential for a wide range of applications from strong-field physics to selectively pump and probe low energy excitations in condensed matter and molecular vibrations. Here we report a four stage optical parametric chirped pulse amplifier (OPCPA) which generates ultrashort pulses at a central wavelength of 3000 nm with 430 μJ energy per pulse at a bandwidth of 490 nm. Broadband emission of a Ti:sapphire oscillator seeds synchronously the four OPCPA stages at 800 nm and the pump line at 1030 nm. The first stage amplifies the 800 nm pulses in BBO using a non-collinear configuration. The second stage converts the wavelength to 1560 nm using difference frequency generation in BBO in a collinear geometry. The third stage amplifies this idler frequency non-collinearly in KTA. Finally, the fourth stage generates the 3000 nm radiation in a collinear configuration in LiIO_3 due the broad amplification bandwidth this crystal provides. We compress these pulses to 65 fs by transmission through sapphire. Quantitative calculations of the individual non-linear processes in all stages verify that our OPCPA architecture operates close to optimum efficiency at minimum absorption losses, which suggests that this particular design is very suitable for operation a high average power at multi kHz repetition rates.

© 2019 Optical Society of America under the terms of the [OSA Open Access Publishing Agreement](#)

1. Introduction

Development of high power femtosecond laser sources in the MIR range is of high practical interest. On the one hand, this holds for the physics of strong field interactions, because the ponderomotive energy of electrons in the laser field increases quadratically with the laser wavelength. This brings about new possibilities in particle acceleration [1, 2], high order harmonic generation in gases [3, 4] and solids [5], attosecond electronics [6], and K_α x-ray generation [7]. On the other hand, femtosecond MIR pulses are essential for time resolved spectroscopy of molecules in gas phase and condensed matter in general. Combined with the above mentioned high harmonic generation MIR pulses also offer a unique possibility of carrying out complimentary pump-probe measurements both in the infrared and soft x-ray spectral range.

Well-established sources of femtosecond pulses in the MIR range are optical parametric oscillators (OPOs) and amplifiers (for the laser MIR sources see [8] and references therein). OPOs synchronously pumped by mode locked Ti:sapphire lasers work at high repetition rates (about 100 MHz) and deliver relatively low energy pulses (below 1 nJ) [9, 10]. Pulse energies on a microjoule (or even tens of microjoules) level can be achieved with sources utilizing Ti:sapphire or Yb:KGW systems with the repetition rates of about 1 kHz [6, 11–14]. Switching from this "short pulse" parametric generation to the OPCPA technique [15] allows much higher average power and/or pulse energy using, e.g., picosecond Yb^{3+} or Nd^{3+} pump lasers. In [16], for example, 42 fs pulses at the wavelength of 3400 nm with the energy of 12 μJ were generated at the repetition rate of 50 kHz (see also [17, 18]). At the repetition rate of 1 kHz energy of 1 mJ at the wavelength of 5 μm was reached [19]. Energies up to 20 mJ at the repetition rate of 20 Hz were demonstrated in [20] (see also [21]). Compared to conventional laser amplifiers

high power OPCPA also benefit from much lower thermal load of the amplifying medium.

Several crystals (e.g. LiNbO_3 , KNbO_3 , LiIO_3 , KTA, RTA) support bandwidths needed for sub- 100 fs MIR pulse generation. The largest bandwidths are achieved making use of noncollinear optical parametric amplification (NOPA) [22,23], where the large bandwidth of the signal is achieved by introducing an angular chirp to the idler wave. However, the chirp has to be avoided at the stage, where the MIR radiation is generated as an idler. This makes the choice of a suitable crystals challenging¹. In [16] the broadband amplification (about 400 nm bandwidth with the central wavelength of 3400 nm) was achieved using aperiodically poled $\text{MgO}:\text{LiNbO}_3$ (see also [27–30]). In [20] the authors make use of a remarkably wide bandwidth of the collinear conversion in KTA type II interaction at the wavelength of 3900 nm by pumping at the wavelength of about 1000 nm. Unfortunately, KTA crystals start to absorb at the wavelengths longer than 3500 nm [31], which may lead to limitations in high-repetition-rate systems due to thermal distortions [32, 33].

In this paper we report an OPCPA system producing sub-70 fs pulses at the wavelength of 3000 nm with the pulse energy of 430 μJ at a repetition rate of 100 Hz. Our experimental measurements are supported by calculations using a specially developed split-step 2D Matlab code.

2. Experimental

The OPCPA architecture is depicted in Fig. 1. The system is seeded by a Ti:sapphire (Ti:Sa) oscillator producing 6 fs pulses at the central wavelength of 800 nm with the energy of 2.5 nJ per pulse and the repetition rate of 80 MHz. The pulse duration was measured directly after the laser output using SPIDER. The spectrum of the Ti:Sa oscillator is presented in the inset to Fig. 1. A fraction of the emission at the wavelength of 1030 ± 2 nm is used to seed the OPCPA pump channel.

2.1. Pump channel

The above mentioned narrow band Ti:Sa emission at 1030 nm with 30 pJ/pulse passes through an electro optical modulator (EOM), which reduces the pulse repetition rate down to 20 MHz. After a fiber pre-amplifier the pulses with the energy of about 1 nJ are stretched to the duration of about 2 ns. The stretched pulses are amplified in a two stage amplifier with the maximum repetition rate of 300 kHz: a commercial regenerative Yb:KGW amplifier (Amplitude Systems) and subsequently in an Innoslab [34] power amplifier (Amphos GmbH). The maximum average output power of the pump channel reaches 400 W at repetition rates from about 20 to 300 kHz. In the present work the repetition rate was 100 Hz. The output pulses with the energy of 20 mJ are compressed to the duration of 1.2 ps. For the stretching and recompression multilayer dielectric gratings (LLNL) with the line density of 1740 1/mm at the angle of incidence of 57° are used. The effective grating distance is 4 m in a folded stretcher and compressor geometry. A 1 mJ fraction of the compressed pulse energy with a flat top spatial profile is frequency doubled in a 2 mm LBO crystal. The crystal is heated to 190°C in order to achieve non-critical phase matching. The second harmonic (SH) pulses at the wavelength of 515 nm with the energy of 700 μJ is used to pump the first two OPCPA stages as indicated in Fig. 1.

2.2. OPCPA

The seed pulses provided by the Ti:Sa oscillator are amplified in the first stage in a 3.9 mm thick type I BBO crystal ($\theta = 24.3^\circ$). The interaction is non-collinearly phase matched with the angle of 2.4° between the pump and the seed beams. Before amplification the 6 fs pulses are stretched with the help of a 10 cm BK7 slab to the duration of 3 ps full width at half maximum (FWHM),

¹In [24–26] some methods of correction for the idler chirp after NOPA stages have been demonstrated.

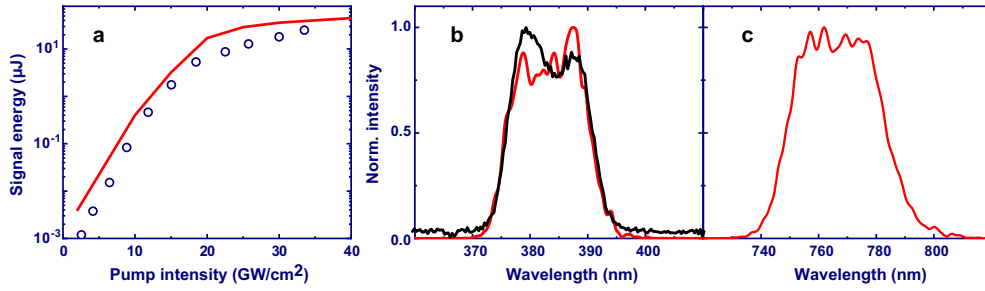


Fig. 2: Calculated (red line) and measured (open circles) output energy of the first OPCPA stage (a). Experimental (dashed line) and calculated (red solid line) SH spectra are shown in panel (b). The calculated spectrum of the signal is shown in panel (c).

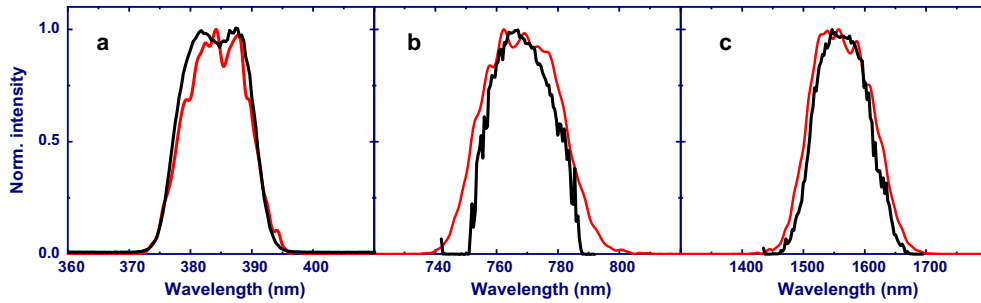


Fig. 3: Second OPCPA stage: calculated (red solid lines) and measured (dashed line) spectra of the SH of the signal pulse (a), of the signal (b) and of the idler (c), respectively.

ground stemming from unamplified seed pulses at high repetition rate (80 MHz). This background was suppressed by conversion of the signal to the SH using a $60 \mu\text{m}$ BBO crystal. The SH spectrum was measured using a grating spectrometer with a CCD (charge coupled device) camera. The SH spectrum together with the calculated one as well as the corresponding calculated signal spectrum are presented in Fig. 2b and 2c. Due to good agreement between the two SH spectra in 2b, we assume that the real signal spectrum is indeed close to the one drawn in Fig. 2c. Its bandwidth of about 35 nm FWHM supports 30 fs pulses.

Now we turn to the second OPCPA stage. A 0.6 mm type I BBO ($\theta = 22.5^\circ$) crystal is seeded by the signal wave of the first OPCPA stage and is used in the difference frequency generation (DFG). The pump and the signal beams are interacting collinearly in order to avoid the angular chirp of the idler wave. The diameters of both beams are 0.6 mm FWHM. With the pump and the seed pulse energies of $400 \mu\text{J}$ and $6 \mu\text{J}$, respectively, the output energy at the central wavelength of 1560 nm is $20 \mu\text{J}$. The corresponding measured and calculated spectra are presented in Fig. 3. The scanning monochromator coupled with an InGaAs photodiode was used for the spectral measurements. The measured spectral width (FWHM) of the idler of 105 nm supports 43 fs pulses.

In the third NOPA OPCPA stage a 3 mm thick type II KTA crystal with $\theta = 48.6^\circ$ is used. The stage is seeded by the idler pulses of the second stage with the pulse energy of $15 \mu\text{J}$ at a non-collinearity angle of 4.2° . The output energy at the central wavelength of 1560 nm reached $200 \mu\text{J}$ with a 140 nm bandwidth FWHM using pump pulses with the energy of 1.5 mJ. The corresponding spectra can be seen in Fig. 4. The SH and the IR spectra were measured using the spectrometer with the CCD camera and the scanning monochromator with the InGaAs photodiode, respectively.

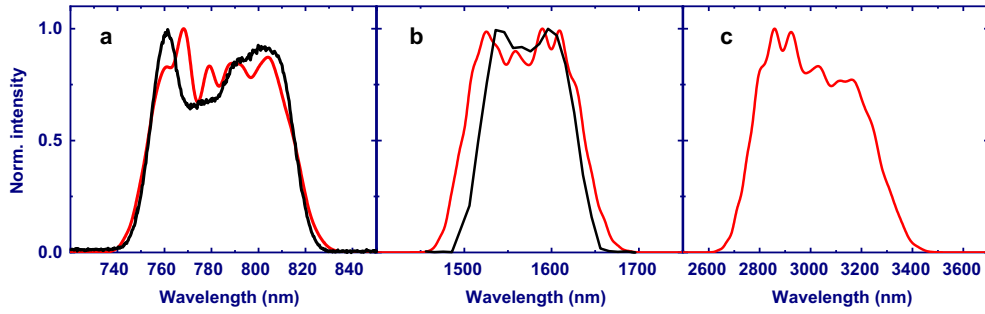


Fig. 4: Third OPCPA stage: Calculated (red solid lines) and measured (black dashed lines) spectra of the SH of the signal pulse (a) and of the signal pulse (b). The calculated idler spectrum (c) is wide enough to support sub 40 fs pulses.

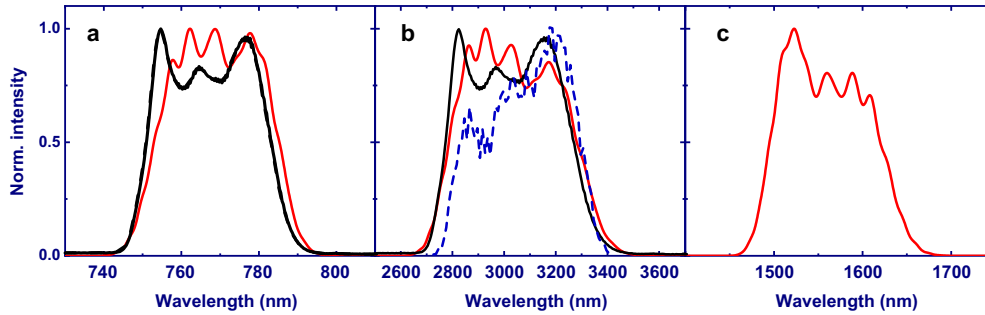


Fig. 5: Calculated (red solid lines) and measured (black dashed lines) spectra after the fourth stage. Spectrum of the idler pulse up-converted in a thin KTA crystal using pump at 1030 nm (a). Spectra of the idler (b) and signal (c).

The fourth and last OPCPA stage is used to shift the wavelength to the MIR range. A 4 mm thick type I LiIO_3 crystal, $\theta = 19^\circ$ is pumped with 9 mJ pulses at the wavelength of 1030 nm. With the seed energy of 200 μJ at 1560 nm the output energy of the idler at 3000 nm reaches 430 μJ . The LiIO_3 crystal was chosen because its wide amplification bandwidth in collinear geometry. The corresponding spectra are presented in Fig. 5. They were measured using frequency up conversion in a thin KTA crystal. For the up conversion we used pump pulses at the wavelength of 1030 nm. The spectra of the resulting frequency shifted pulses were centered around 770 nm. Unlike the case of the SH generation, the measured up converted spectra can be directly mapped to the MIR range (Fig. 5b). This is possible, because the pump spectral width (1.7 nm FWHM) is much smaller and the pulse duration (1.2 ps) longer compared to those of the idler. In order to check the validity of this measurement we have also measured the idler spectrum using a monochromator with a PbSe photodiode (Fig. 5b, blue dashed line). It can be seen that the directly measured MIR spectrum is cut in the vicinity of 2700-2800 nm. The beam path from the last OPCPA stage to the monochromator is about 3 meters, so this cut can be attributed to the water vapor absorption. The up conversion method delivers an unperturbed spectrum, because the up conversion KTA crystal is placed immediately after the LiIO_3 crystal. Another advantage of the up conversion is that the spectra are recorded using a conventional CCD camera practically in a "single shot" mode, which makes the alignment much easier. The idler pulse duration (<500 fs) can be estimated from the autocorrelation measurement of the signal pulse (see Fig. 6a).

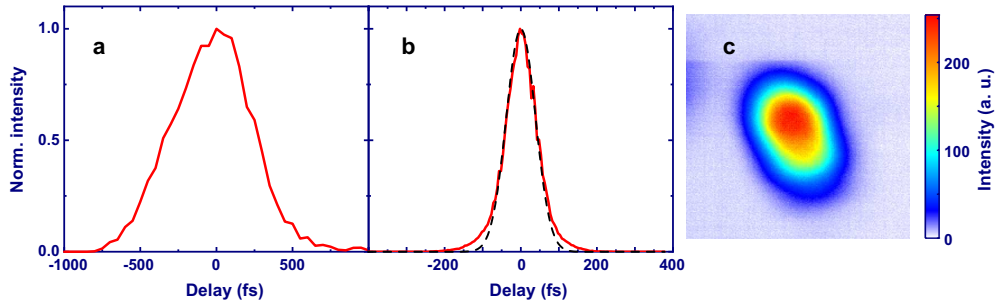


Fig. 6: Second order AC trace of uncompressed signal pulses at the wavelength of 1560 nm (a) and of the compressed MIR pulses at the wavelength of 3000 nm (b), red solid curve. Black dashed line in (b) corresponds to a Gaussian function with 90 fs FWHM. Panel (c) shows the intensity distribution in the 3000 nm beam (recorded using a DataRay camera WinCamD-IR-BB).

According to Fig. 5b the bandwidth of the 3000 nm pulses exceeds 490 nm FWHM. This bandwidth supports 35 fs pulse duration, if properly compressed. In this work we have used a simple compression using sapphire plates to compensate only for the second order dispersion. A second order autocorrelation (AC) function using a 0.5 cm sapphire plate is presented in Fig. 6b. From the measured AC width of 90 fs (FWHM) we estimate the pulse duration to be about 65 fs using the deconvolution factor of 1.4 for Gaussian pulses. In all the stages the calculated B-integral at maximum intensity was below $\pi/4$, assuming the nonlinear refraction index \tilde{n}_2 to be 8×10^{-16} , 17×10^{-16} , and $\leq 20 \times 10^{-16}$ cm²/W for BBO, KTA, and LiIO₃, respectively. The intensity distribution in the 3000 nm beam taken at 1 m distance from the LiIO₃ crystal with the help of an infrared CCD camera is shown in Fig. 6c.

3. Conclusions and outlook

In summary, we report an OPCPA system generating 430 μ J pulses at the wavelength of 3000 nm with the bandwidth of 490 nm FWHM and the repetition rate of 100 Hz. Using a simple bulk compressor the pulses were compressed to the duration of about 65 fs. The reported pulse bandwidth supports 35 fs pulses, which can be probably achieved by compensation of higher order dispersion.

The combination of BBO, KTA, and LiIO₃ crystals in the four OPCPA stages allows keeping a broad bandwidth at the center wavelength of 3000 nm with little absorption in the crystals. KTA and LiIO₃ crystals are available with relatively low absorption at the pump wavelength ($\alpha_{KTA} \approx 0.01$ %/cm [32]) and $\alpha_{LiIO_3} < 0.02$ %/cm [37]). This may allow MIR pulse production with much higher repetition rates and average powers, e.g. average power >5 W is achievable at the repetition rate of 20 kHz keeping the same pulse energy.

4. Funding

We acknowledge financial support by the Deutsche Forschungsgemeinschaft through SFB 1242 (project number 278162697, TP A05).

5. Acknowledgments

We thank Frank Meyer for his experimental support and initial development of the Matlab code. We are also very grateful to A. Baltuška, A. Pugžlys, and S. Ališauskas for their valuable help in early stages of the work.

References

1. T. Tajima and J.M. Dawson, "Laser electron accelerator," *Phys. Rev. Lett.* **43**, 267–270 (1979).
2. D. Woodbury, L. Feder, V. Shumakova, C. Gollner, R. Schwartz, B. Miao, F. Salehi, A. Korolov, A. Pugžlys, A. Baltuška, and H. M. Milchberg, "Powerful femtosecond pulse generation by chirped and stretched pulse parametric amplification in BBO crystal," *Opt. Lett.* **43**, 1131–1134 (2018).
3. T. Popmintchev, M.-C. Chen, A. Bahabad, M. Gerrity, P. Sidorenko, O. Cohen, I. Christov, M. Murnane, and H. Kapteyn, "Phase matching of high harmonic generation in the soft and hard X-ray regions of the spectrum," *PNAS* **106**, 10,516–10,521 (2009).
4. T. Popmintchev, M.-C. Chen, D. Popmintchev, P. Arpin, S. Brown, S. Ališauskas, G. Andriukaitis, T. Balčiūnas, O. Mücke, A. Pugžlys, A. Baltuška, B. Shim, S. Schrauth, A. Gaeta, C. Hernández-García, L. Plaja, A. Becker, A. Jaron-Becker, M. Murnane, and H. Kapteyn, "Bright Coherent Ultrahigh Harmonics in the keV X-ray Regime from Mid-Infrared Femtosecond Lasers," *Science* **336**, 1288–1291 (2012).
5. M. T. Hassan, T. T. Luu, A. Moulet, O. Raskazovskaya, P. Zhokhov, M. Garg, N. Karpowicz, A. M. Zheltikov, V. Pervak, F. Krausz, and E. Goulielmakis, "Optical attosecond pulses and tracking the nonlinear response of bound electrons," *Nature* **530**, 66–70 (2016).
6. G. Vampa, T. J. Hammond, B. E. S. N. Thiré and, F. Légaré, C. R. McDonald, T. Brabec, and P. B. Corkum, "Linking high harmonics from gases and solids," *Nature* **522**, 462–464 (2015).
7. J. Weisshaupt, V. Juvé, M. Holtz, S. Ku, M. Woerner, T. Elsaesser, S. Ališauskas, A. Pugžlys, and A. Baltuška, "High-brightness table-top hard X-ray source driven by sub-100-femtosecond mid-infrared pulses," *Nature Photon.* **8**, 927–930 (2014).
8. P. Komm, U. Sheintop, S. Noach, and G. Marcus, "Carrier-to-envelope phase-stable, mid-infrared, ultrashort pulses from a hybrid parametric generator: Cr:ZnSe laser amplifier system," *Opt. Express* **27**, 18,522–18,532 (2019).
9. D. E. Spence, S. Wielandy, and C. L. Tang, "High average power, high-repetition rate femtosecond pulse generation in the 1–5 μm region using an optical parametric oscillator," *Appl. Phys. Lett.* **68**, 452–454 (1996).
10. C. McGowan, D. Reid, M. Ebrahimzadeh, and W. Sibbett, "Femtosecond pulses tunable beyond 4 μm from a KTA-based optical parametric oscillator," *Opt. Commun.* **134**, 186–190 (1997).
11. V. Petrov, F. Noack, and R. Stolzenberger, "Seeded femtosecond optical parametric amplification in the mid-infrared spectral region above 3 μm ," *Appl. Opt.* **36**, 1164–1172 (1997).
12. R. A. Kaindl, M. Wurm, K. Reimann, P. Hamm, A. M. Weiner, and M. Woerner, "Femtosecond pulses tunable beyond 4 μm from a KTA-based optical parametric oscillator," *J. Opt. Soc. Am. B* **17**, 2086–2094 (2000).
13. D. Brida, C. Manzoni, G. Cirmi, M. Marangoni, S. D. Silvestri, and G. Cerullo, "Generation of broadband mid-infrared pulses from an optical parametric amplifier," *Opt. Express* **15**, 15,035–15,040 (2007).
14. N. Ishii, P. Xia, T. Kanai, and J. Itatani, "Optical parametric amplification of carrier-envelope phase-stabilized mid-infrared pulses generated by intra-pulse difference frequency generation," *Opt. Express* **27**(8), 11,447–11,454 (2019).
15. A. Dubietis, G. Jonušauskas, and A. Piskarskas, "Powerful femtosecond pulse generation by chirped and stretched pulse parametric amplification in BBO crystal," *Opt. Commun.* **88**, 437–440 (1992).
16. B. W. Mayer, C. R. Phillips, L. Gallmann, M. M. Fejer, and U. Keller, "Sub-four-cycle laser pulses directly from a high-repetition-rate optical parametric chirped-pulse amplifier at 3.4 μm ," *Opt. Lett.* **38**, 4265–4268 (2013).
17. T. Kanai, Y. Lee, M. Seo, and D. E. Kim, "Supercontinuum-seeded, carrier-envelope phase-stable, 4.5-W, 3.8 μm , 6-cycle, KTA optical parametric amplifier driven by a 1.4-ps Yb:YAG thin-disk amplifier for nonperturbative spectroscopy in solids," *J. Opt. Soc. Am. B* **36**(9), 2407–2413 (2019).
18. B. M. Luther, K. M. Tracy, M. Gerrity, S. Brown, and A. T. Krummel, "2D IR spectroscopy at 100 kHz utilizing a Mid-IR OPCPA laser source," *Opt. Express* **24**(4), 4117–4127 (2016).
19. M. Bock, L. von Grafenstein, U. Griebner, and T. Elsaesser, "Generation of millijoule few-cycle pulses at 5 μm by indirect spectral shaping of the idler in an optical parametric chirped pulse amplifier," *J. Opt. Soc. Am. B* **35**(12), C18–C24.
20. V. Shumakova, P. Malevich, S. Ališauskas, A. Voronin, A. Zheltikov, D. Faccio, D. Kartashov, A. Baltuška, and A. Pugžlys, "Multi-millijoule few-cycle mid-infrared pulses through nonlinear self-compression in bulk," *Nat. Commun.* **7**, 12,877 (2016).
21. G. Andriukaitis, T. Balčiūnas, S. Ališauskas, A. Pugžlys, A. Baltuška, T. Popmintchev, M.-C. Chen, M. Murnane, and H. Kapteyn, "90 GW peak power few-cycle mid-infrared pulses from an optical parametric amplifier," *Opt. Lett.* **36**, 2755–2757 (2011).
22. S. Witte and K. Eikema, "Ultrafast Optical Parametric Chirped-Pulse Amplification," *IEEE J. Sel. Topics Quantum Electron.* **18**, 296–307 (2013).
23. J. Zheng and H. Zacharias, "Non-collinear optical parametric chirped-pulse amplifier for few-cycle pulses," *Appl. Phys. B* **97**, 765–779 (2009).
24. A. Shirakawa, I. Sakane, and T. Kobayashi, "Pulse-front-matched optical parametric amplification for sub-10-fs pulse generation tunable in the visible and near infrared," *Opt. Lett.* **23**, 1292–1294 (1998).
25. S.-W. Huang, J. Moses, and F. Kärtner, "Broadband noncollinear optical parametric amplification without angularly dispersed idler," *Opt. Lett.* **37**, 2796–2798 (2012).
26. O. Isaienko and E. Borguet, "Pulse-front matching of ultrabroadband near-infrared noncollinear optical parametric amplified pulses," *J. Opt. Soc. Am. B* **26**, 965–972 (2009).

27. N. Bigler, J. Pupeikis, S. Hrisafov, L. Gallmann, C. R. Phillips, and U. Keller, "High-power OPCPA generating 1.7 cycle pulses at $2.5\ \mu\text{m}$," *Opt. Express* **26**(20), 26,750–26,757 (2018).
28. N. Thiré, R. Maksimenka, B. Kiss, C. Ferchaud, G. Gitzinger, T. Pinoteau, H. Joussetin, S. Jarosch, P. Bizouard, V. D. Pietro, E. Cormier, K. Osvay, and N. Forget, "Highly stable, 15 W, few-cycle, 65 mrad CEP-noise mid-IR OPCPA for statistical physics," *Opt. Express* **26**(21), 26,907–26,915 (2018).
29. X. Zou, W. Li, H. Liang, K. Liu, S. Qu, Q. J. Wang, and Y. Zhang, "300 μJ , 3 W, few-cycle, 3 μm OPCPA based on periodically poled stoichiometric lithium tantalate crystals," *Opt. Lett.* **44**(11), 2791–2794 (2019).
30. P. Rigaud, A. V. de Walle, M. Hanna, N. Forget, F. Guichard, Y. Zaouter, K. Guesmi, F. Druon, and P. Georges, "Supercontinuum-seeded few-cycle mid-infrared OPCPA system," *Opt. Express* **24**, 26,494–26,502 (2016).
31. G. Hansson, H. Karlsson, S. Wang, and F. Laurell, "Transmission measurements in KTP and isomorphous compounds," *Appl. Opt.* **39**, 5058–5069 (2000).
32. K. Mecseki, M. K. R. Windeler, M. J. Prandolini, J. S. Robinson, J. M. Fraser, A. R. Fry, and F. Tavella, "High-power dual mode IR and NIR OPCPA," in *Proc. SPIE 11033, High-Power, High-Energy, and High-Intensity Laser Technology IV*, J. Hein and T. J. Butcher, eds., p. 110330I (2019).
33. K. Mecseki, M. K. R. Windeler, A. Miahnahri, J. S. Robinson, J. M. Fraser, A. R. Fry, and F. Tavella, "High average power 88 W OPCPA system for high-repetition-rate experiments at the LCLS x-ray free-electron laser," *Opt. Lett.* **44**, 1257–1260 (2019).
34. P. Russbuedt, T. Mans, G. Rotarius, J. Weitenberg, H. Hoffmann, and R. Poprawe, "400 W Yb:YAG Innoslab fs-amplifier," *Opt. Express* **17**, 12,230–12,245 (2009).
35. S. Hädrich, J. Rothhardt, M. Krebs, S. Demmler, J. Limpert, and A. Tünnermann, "Improving carrier-envelope phase stability in optical parametric chirped-pulse amplifiers by control of timing jitter," *Opt. Lett.* **37**, 4910–4912 (2012).
36. F. J. Furch, A. Giree, F. Morales, A. Anderson, Y. Wang, C. P. Schulz, and M. J. J. Vrakking, "Close to transform-limited, few-cycle 12 μJ pulses at 400 kHz for applications in ultrafast spectroscopy," *Opt. Express* **24**, 19,293–19,310 (2016).
37. D. J. Gettemy, W. C. Harker, G. Lindholm, and N. P. Barnes, "Some Optical Properties of KTP, LiIO_3 , and LiNbO_3 ," *IEEE J. of QE* **24**, 2231–2237 (1988).